



ORIGINAL ARTICLE

A novel high performance stopped-flow apparatus equipped with a special constructed mixing chamber containing a plunger under inert condition with a very short dead-time to investigate very rapid reactions



Sayyed Mostafa Habibi Khorassani ^{a,*}, Ali Ebrahimi ^a,
Malek Taher Maghsoodlou ^a, Mehdi Shahraki ^a, Dennice Price ^b, Ali Paknahad ^a

^a Department of Chemistry, Faculty of Science, The University of Sistan and Baluchestan, Zahedan, P.O. Box 98135-674, Zahedan, Iran

^b Department of Chemistry and Applied Chemistry, The University of Salford, Salford, UK

Received 27 December 2010; accepted 16 February 2011
Available online 22 February 2011

KEYWORDS

Stopped-flow instrument;
Rapid reaction;
Rate constant;
Dead-time;
Mixing efficiency

Abstract The present work set out to establish a novel stopped-flow instrument equipped with a special constructed mixing chamber containing a plunger to enable a kinetic study of the very rapid reactions under a dry inert atmosphere glove bag, in particular, for the reactions are sensitive to moisture or air. A stopped-flow spectrophotometer is essentially a conventional spectrophotometer with the addition of a system for rapid mixing of solutions. The purpose of this work is to describe the fabrication and evaluation of specially constructed and in-expensive stopped-flow system. The evaluation includes determination of the dead-time, relative mixing efficiency, and the measurement of known rate constants. Herein, a dead-time of about 3.4 ms was determined in the final modified construction of the stopped-flow apparatus in order to investigate the rapid initial during which some form of reaction intermediate is presented to be formed.

© 2011 Production and hosting by Elsevier B.V. on behalf of King Saud University.

* Corresponding author. Tel./fax: +98 541 2446565.
E-mail address: smhabibikhorassani@yahoo.com (S.M.H. Khorassani).
Peer review under responsibility of King Saud University.



Production and hosting by Elsevier

1. Introduction

A stopped-flow apparatus was constructed by Roughton and Hartridge to measure the rate of binding of carbon monoxide to haemoglobin (Hartridge and Roughton, 1923). In 1940, Chance developed a modification of the stopped-flow apparatus (Chance and Franklin, 1940). Improvements were subsequently made by Gibson, Chance, and others (Gibson, 1966;

Gibson and Greenwood, 1963). Several types of rapid scan stopped-flow apparatus have been made, using rapid scanning monochromators (Dye and Feldman, 1966; Wightman et al., 1974; Coolen et al., 1975; Paradakis et al., 1975; Suelter et al., 1975), a Vidicon (Milano and Pardue, 1975; Ridder and Margerum, 1977) and a special photo-tube called an "image dissector" and digital memory circuits (Nakamura, 1971).

Recently a silicon photoarray detector has been used in place of the image dissector. When used with a pulsed flash lamp as the light source, this modification can give improvement in the spectral time resolution down to a few microseconds (Brzovic and Dunn, 1995; Yutaka, 1984). By this improvement, rapid kinetic and scanning techniques have been employed to observe the reaction of dioxygen with fully reduced cytochrome oxidase at room temperature following stopped flow laser flash photolysis of the CO compound of the enzyme.

In 1993, at least five companies introduced commercial rapid-scanning stopped-flow (RSSF) UV/visible spectrometer systems which employ either silicon photodiode array detectors (four or five) or a single-element (phototube) detector suitable for use in the study of enzyme catalytic mechanisms (Brzovic and Dunn, 1993). This reaction was investigated by a typical stopped-flow rapid scanning spectrophotometer experiment as follows. 20 μM solution of ferric myoglobin (Mb^+) in the presence of 1 mM KCN was mixed in the Gibson–Durrum stopped-flow apparatus with 1–100 mM sodium dithionite ($\text{Na}_2\text{S}_2\text{O}_4$). The absorption spectrum was recorded (over a 150 nm wavelength range) by means of a rapid scanning photodiode array spectrophotometer adapted to the 2-cm light path cell of the stopped flow apparatus (Andrea et al., 1990).

In a similar work, the rate constant for cyanide dissociation from ferrous parascaris haemoglobin was measured as $k = 0.11 \text{ s}^{-1}$ by this method (Giovanni et al., 1994). A dielectric resonator based electron paramagnetic resonance probe was constructed for stopped-flow kinetic studies (Sienkiewicz et al., 1994). A new high-pressure stopped-flow apparatus equipment enables one to monitor fast reactions in various organic solvents as well as in strongly acidic media (Ishihara et al., 1999). In 2007, a capacitance cell has been designed for stopped-flow measurements of very dilute low-relative permittivity liquid solutions (Tjahjono et al., 2007). In recent year, a combination of microelectrophoresis, laser-trap methodology and stopped-flow techniques were designed to study enzyme kinetics with single molecule sensitivity (Kahl et al., 2009). The stopped-flow apparatus has now become a handy laboratory instrument like a spectrophotometer and it can be handled easily by students and researchers alike. The stopped-flow method is one of the most used of the modern techniques for studying fast reactions in solution. The performance of the apparatus and the detection methods are being further improved and extended. At the same time, the fields of application are also being broadened to include many biochemical analyses. The evaluation of rate constants might at first glance be thought somewhat troublesome for those not used to kinetic procedures. However, recent developments in microcomputers have enabled first-order rate constant data to be available immediately following measurement.

The stopped-flow method is confidently expected to become an even more widely used technique especially in biochemical analysis. Herein, we set out to improve the instrument config-

uration in order to investigate the rapid initial during which some form of reaction intermediate is presented to be formed and we now describe the construction of high performance stopped-flow apparatus specially designed for this purpose.

2. Apparatus and chemicals

The digital oscilloscope Model Lecroy 9400 dual 125MHz was used with a Hewlett Packard plotter. Stopped-flow spectrophotometer which is presented in the following sections, initially the plunger, containing the mixing chamber, was designed to fit into a $10 \times 10 \times 45 \text{ mm}$ spectrophotometer cell according to the structure illustrated in Fig. 2.

All chemicals were of analytical reagent grade. The concentrations used were $5 \times 10^{-2} \text{ M}$ for the 99% L-ascorbic acid obtained from Sigma and $5 \times 10^{-4} \text{ M}$ for the 98% 2,6-dichlorophenolindophenol obtained from Fisher. Both the reactants were in 0.10 M sodium phosphate buffer solution that was prepared by dissolving the 99.999% sodium dihydrogen phosphate (Aldrich) in the 99.99% sodium hydroxide obtained from Aldrich.

3. Results and discussion

3.1. Fluid delivery system

The fluid delivery system is a modification of a design published by Strittmatter (Gibson et al., 1964), and the principal features of the syringe pushing block are shown in Fig. 1. Its operation can be described as follows: the reactants are drawn into each syringe through the polyethylene tubing (A) from the filling valves (B). The flow from the two syringes (C) which contain the reactant solutions is initiated by movement of the pushing block (D) which is operated manually. Rapid, smooth mixing of the reactants, prior to their entry into the reaction cell, can be obtained by an experienced operator. However, on many instruments, the pushing block is operated by a pneumatic or hydraulic system and this is probably better for inexperienced operators. The solutions then flow into the mixing chamber through the polyethylene tubes (E), from each

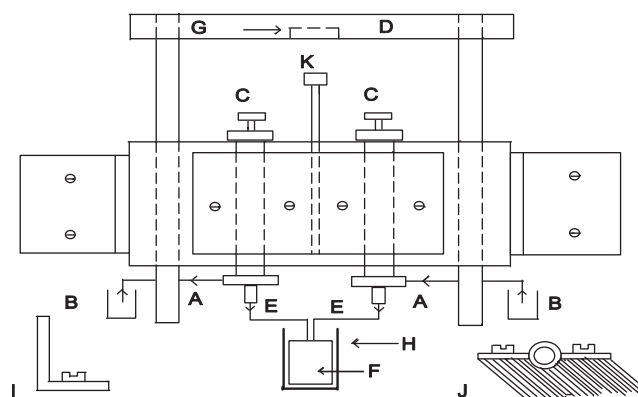


Figure 1 Syringes and driving block. A, Polyethylene tube. B, Reservoirs. C, Insulin syringes. D, Pushing block. E, Polyethylene tube over the external portion of the needles of the plunger. F, Teflon plunger. G, Trigger micro switch. H, Spectrophotometric cell. I, Fastenings to base board. J, Fastening for syringes. K, Brass stop on the threaded rod.

syringe which is placed over the external portion of the stainless steel needles of the plunger (F).

The essential feature of the present stopped-flow apparatus is that the mixing chamber is contained within the plunger that fits into a spectrophotometer cell. The details of the plunger, containing the mixing chamber, are shown in Fig. 2.

The Teflon plunger (A) is shaped to fit into a $10 \times 10 \times 45$ mm UV spectrophotometer cell. The two inlet vertical channels (B) at the top are 0.5 mm in diameter for approximately 8 mm to accommodate short sections of stainless steel syringe needles (C). These channels lead directly to mixing chamber (D) which is the horizontal channel, 0.5 mm in diameter, and perpendicular to the vertical inlet channels. A plug (E) is inserted to seal-off the horizontal channel. A short channel (F) at the bottom of the mixing chamber, 0.5 mm in diameter, provides the exit to the bottom of the plunger. The mixed solution which exits from the bottom of the plunger causes the plunger to rise. The positions of the plunger in the spectrophotometer cell are shown before and after mixing in Figs. 3 and 4, respectively.

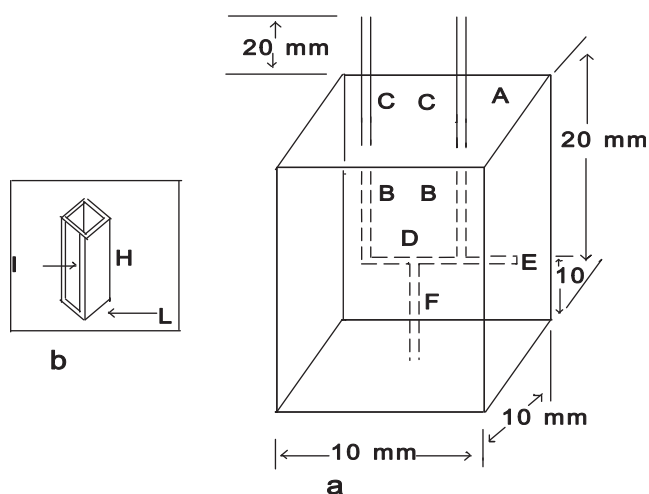


Figure 2 The construction detail of the plunger containing the mixing chamber shown with the spectrophotometer cell. (a) A, Teflon plunger. B, Vertical inlet channels. C, External section of stainless steel needles. D, Mixing chamber. E, Plug. F, Exit channel. (b) I, 10 mm internal width of cell. L, 10 mm path length cell. H, Height of cell, 45 mm.

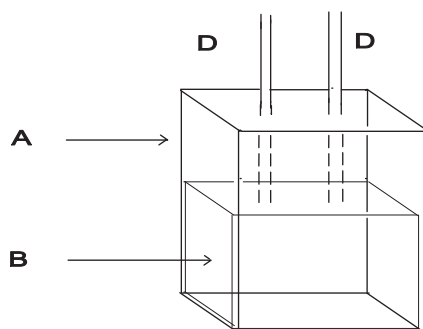


Figure 3 The position of the plunger in the spectrophotometer cell before mixing. A, Spectrophotometer cell. B, Plunger. D, External section of stainless steel needles.

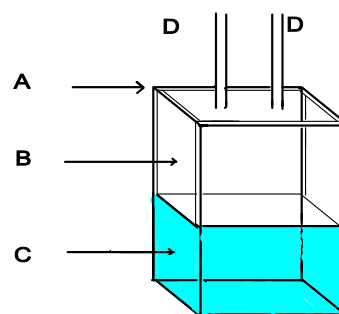


Figure 4 The position of the plunger in the spectrophotometer cell after mixing. A, Spectrophotometer cell. B, Plunger. C, Observation region containing freshly mixed solution. D, External section of stainless steel needles.

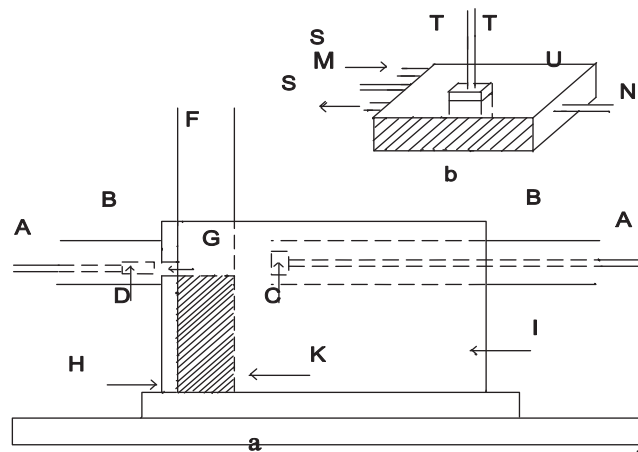


Figure 5 Cell housing with LED and photodiode holder. (a) Inside the cell housing: A, Electrical leads. B, Brass tube. C, Photodiode detector. D, LED source (λ 580 nm, width at half height 29 nm). F, Spectrophotometer cell. G, Circular hole 2.5 mm in diameter. H, Mask with circular hole to restrict light. I, Aluminium block containing the photodiode. K, Metal block which fits the cell holder to locate the cell. J, Metal base. (b) The top of the cell housing: N, photodiode circuit. M, LED supply. S, Tubes for water circulation. T, Section of the polyethylene tube over the external portion of the needles of the plunger. U, The metal box housing the cell. The box has a movable window.

The reaction mixture thus appears in the observation cell, at the bottom of the spectrophotometer cell very shortly after mixing. The light from a yellow LED which is held in the cell housing (Fig. 5) with aluminium block, passes through a slit of width between 2 and 2.5 mm, and is focused on the observation cell. The instrument described in this work is designed for transmission/absorption measurements. However, the geometric arrangement of the observation cell allows monitoring of rapid reactions by several optical parameters. For example, the optical components may be arranged for fluorometric measurements when emitted light is monitored at 90° to the light source.

In this work, the observation cell is used for transmittance/absorption measurements by monitoring the light emerging at 180° to the LED source. The change in transmittance of light passing through the cell is detected by the photodiode. The dimensions (mm) and spectral sensitivity of the BPW21

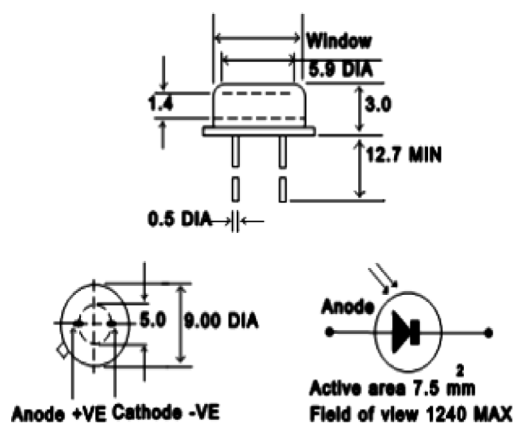


Figure 6 Dimensions (mm) and spectral sensitivity of the BPW21 photodiode (RS Components Ltd.).

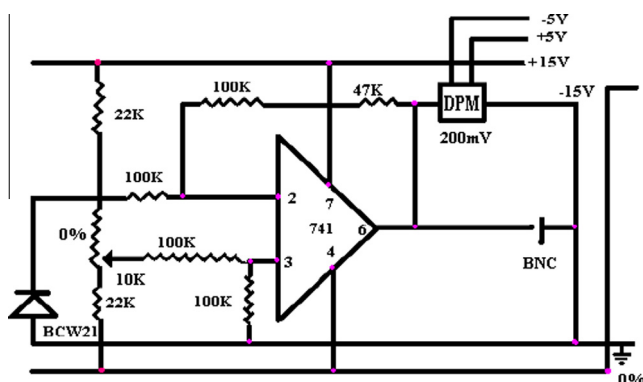
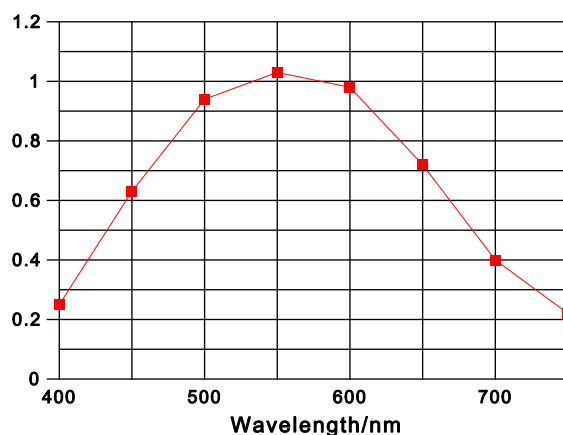


Figure 7 Amplifier and photodiode circuit diagram.

photodiode used in this work are shown in Fig. 6. The photocurrent generated by the photodiode is converted into a voltage by an operational amplifier. The amplifier and photodiode circuit diagram are illustrated in Fig. 7. A trigger micro switch (Fig. 10) initiates the recording of the voltage with time on a digital storage oscilloscope. The reaction curve is down-loaded onto graph paper for subsequent analysis by a printer-recorder attached to the oscilloscope. At the end of each experiment, the plunger is pushed gently down to the bottom of the spectrophotometer cell (Fig. 8), so that the spent solution is forced along the space between the plunger and cell walls to the top from where it is then discarded by removing it with a syringe.

3.2. Performance test

To test the performance of the constructed apparatus the reaction of 2,6-dichlorophenolindophenol (DCPI) by L-ascorbic acid (Tonomura et al., 1978) at pH 5.7 was chosen as an appropriate reaction (Fig. 9) for these reasons: (i) the reaction could be studied under pseudo first order kinetic conditions; (ii) the reaction was accompanied by a significant change in the absorption spectrum; (iii) variation in the reaction velocity was possible when one of the reaction parameters is changed; (iv) in this particular case, the reaction is readily monitored via light absorption without the need for an indicator.

In these experiments the concentrations used were: 5×10^{-2} M for the L-ascorbic acid, 5×10^{-4} M for 2,6-dichlorophenol-indophenol, both the reactants also being in 0.10 M

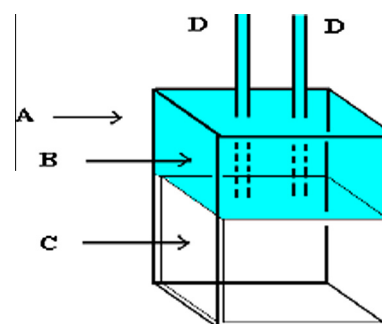


Figure 8 Position of spent solution in the spectrophotometer cell after depressing the plunger. A, Spectrophotometer cell. B, Displaced spent solution. C, Plunger. D, External section of stainless steel needles.

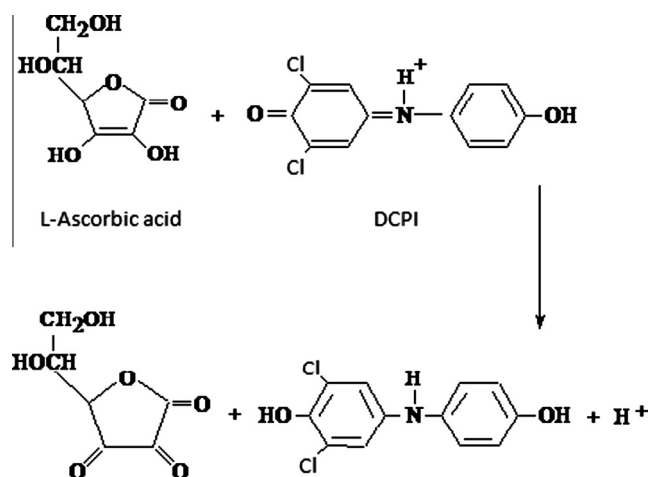


Figure 9 The reduction of 2,6-dichlorophenolindophenol (DCPI) by L-ascorbic acid used as a test reaction for the high-performance stopped-flow apparatus.

phosphate buffer solution. Under these conditions the reductions of DCPI followed pseudo first-order kinetics with respect to the concentration of the DCPI. The rate equation for the reaction between 2,6-dichlorophenolindophenol (DCPI) and L-ascorbic acid may be expressed as:

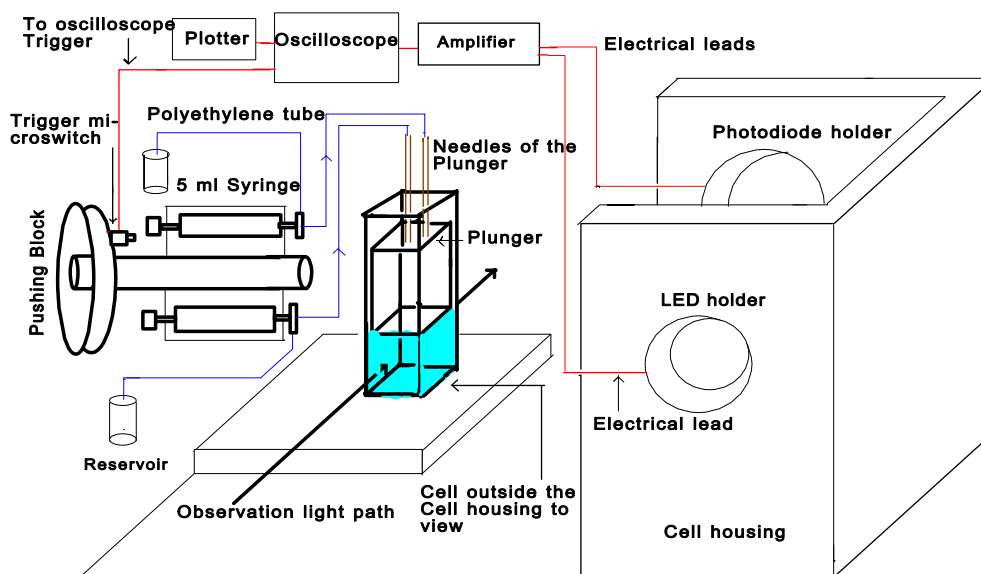


Figure 10 Schematic diagrams of the stopped flow apparatus with oscilloscope monitoring.

$$\text{Rate} = k'[\text{ascorbic acid}][\text{DCPI}]$$

where k' = second order rate constant.

As the experiment uses a large excess of L-ascorbic acid its concentration will remain practically constant throughout the reaction, and rate equation may therefore be expressed as:

$$\text{Rate} = k[\text{DCPI}]$$

$$k = k'[\text{ascorbic acid}]$$

where k = pseudo first order rate constant.

In this condition the reaction follows pseudo first-order kinetics with respect to DCPI according to the integrated rate equation.

$$\log_{10} c_t/c_o = -k \times t/2.303$$

where c_t and c_o are respectively, the actual and initial concentrations of DCPI.

In the photometer equipment the change in reactant concentration is monitored as the change in light absorption by the solution. By reference to the Beer–Lambert law

$$\text{Absorbance } A = \log_{10} I_o/I_t = \xi c l$$

where I_o is the incident light intensity, I_t is the transmittance light intensity, ξ is decadic absorption coefficient, l is the path length, c is reactant concentration.

Thus, since the values of ξ and l are fixed for any particular apparatus/reaction combination.

$$\log_{10} c_t/c_o = \log_{10} A_t/A_o = -k \times t/2.303$$

Thus, the variation of absorbance with time is measured. Then a plot of $\log_{10} A$ as time will be a straight-line of slope $-k/2.303$ and so a value for k can be obtained.

In order to perform test reaction, the apparatus set up is illustrated in Fig. 10. Details of the individual sections were explained earlier. Before the beginning of an experiment the photometer was calibrated to give an approximately zero transmittance signal with the plunger at the bottom of the spectrophotometer cell (no incident light), and an output of

approximately 100% transmittance signal with the plunger at the top of the cell and water in the 10 mm path length spectrophotometer cell (maximum intensity of incident light). The oscilloscope was also set to record data over a suitable period of time and then 0.3 mL of each reactant (L-ascorbic acid and 2,6-dichlorophenolindophenol) solution contained in the two drive syringes was simultaneously injected into the mixing cell. A significant change in absorbance due to the colour change was observed, and the output data were recorded graphically on the oscilloscope screen as voltage against time as the reaction proceeded.

The oscillographic traces obtained were similar to the calibration plot (Fig. 11) obtained for mixing water. It was obvious that practically the whole of the reaction had occurred in the dead time of the apparatus i.e. between the start of the mixing and the first measurement of the light transmission through the mixed solutions. This experimental arrangement therefore had failed to provide suitable data for kinetic analysis.

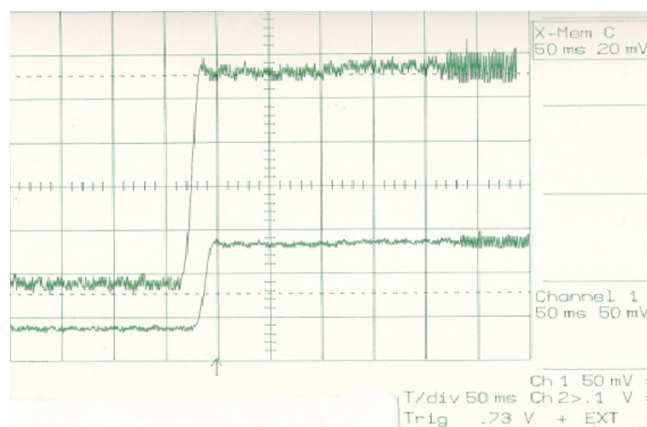


Figure 11 Typical oscillographic picture for the mixing of equal volumes (20 μL) of water, upper trace is a magnification of the lower trace.

3.3. Modified design of the plunger and spectrophotometer cell

These preliminary observations indicated that the dead-time of the initial design of apparatus was too long. In order to reduce the dead-time as much as possible, decreasing the size of the spectrophotometer cell and mixing chamber appeared to be the most practical way. It was therefore decided to modify the configuration of the plunger. Improved design could reduce the amount of reactants that needed to be injected and the time interval between the start of the reaction and the beginning of observation. The modified design of the plunger and micro-spectrophotometer cell are shown in Fig. 12. In this case the modified form of the plunger was shaped to fit into a $10 \times 2 \times 25$ mm micro-spectrophotometer cell. The reaction kinetics was then investigated with just $60 \mu\text{L}$ of each reactant being simultaneously injected into the mixing cell with the conditions as previously described. This experiment enabled a suitable trace to be obtained, which allowed the calculation of the dead-time ($t_0 - t_1$) of the apparatus.

3.4. Determination of the dead-time of the apparatus

To obtain meaningful kinetic measurements it is important to follow measurable changes in reactant with time. If the reaction has half-life comparable to dead time then only half initial concentration of the reactant is left when measurements are begun. Thus the system dead time determines the minimum reaction half-life that can be investigated.

To calculate the dead-time, the difference between the time at which the reaction is started and the time corresponding to the first observation point is measured in ms. Unfortunately, a certain inaccuracy in the determination of the effective start point is always possible because the micro switch always has some mechanical inertia. To overcome these difficulties two experiments at different temperatures (21 and 23°C) were performed with equal volumes of each reactant ($60 \mu\text{L}$) for same reaction with the conditions as previously described. The output data are displayed graphically on the oscilloscope screen as voltage against time in real time as the reaction proceeds e.g. Fig. 13. The procedures for measuring the voltage at various

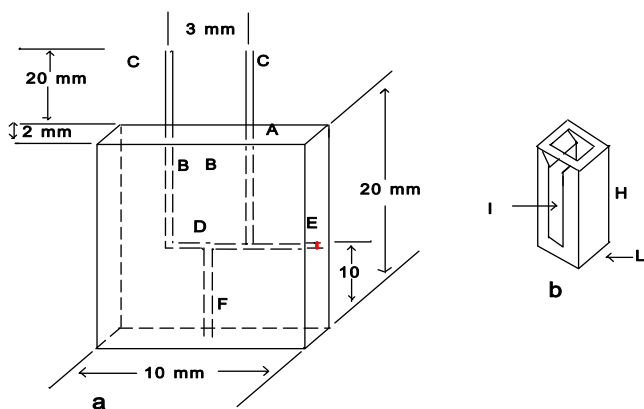


Figure 12 The construction details of the modified design of the plunger containing the mixing chamber shown with the micro spectrophotometer cell. (a) A, Teflon plunger. B, Vertical inlet channel. C, External section of stainless steel needles. D, Mixing chamber. E, Plug. F, Exit channel. (b) I, 2 mm internal width of cell. L, 10 mm path length cell. H, Height of cell, 25 mm.

times recorded by the traces are best understood by reference to simplified sketch in Fig. 14.

Remembering that voltage output (V) from the amplifier is proportional to the light intensity, then $I_t = kV_t + C$ and $I_0 = kV_0 + C$, where k = constant of proportionality, C = constant

But the equipment is pre-set so that output voltage is set to zero when the incident light is blocked off with the plunger at the bottom of the spectrophotometer cell, that is $I_t = 0$ and so $C = 0$ under these circumstances.

$$kV_0/kV_t = I_0/I_t$$

$$\log_{10}(V_0/V_t) = \log_{10}(I_0/I_t) = \epsilon[c]l = \text{absorbance} = A$$

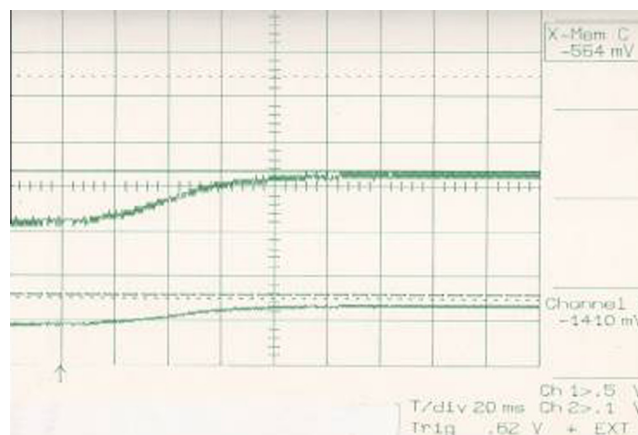


Figure 13 Typical oscillographic picture, upper trace corresponding to the reduction of 5.0×10^{-4} M DCPI by 5.0×10^{-2} M L-ascorbic acid when $60 \mu\text{L}$ of each reactant was mixed at 23°C and pH 5.7, both the reactants being in 0.1 M phosphate buffer. Lower trace corresponds to the same reaction at 21°C .

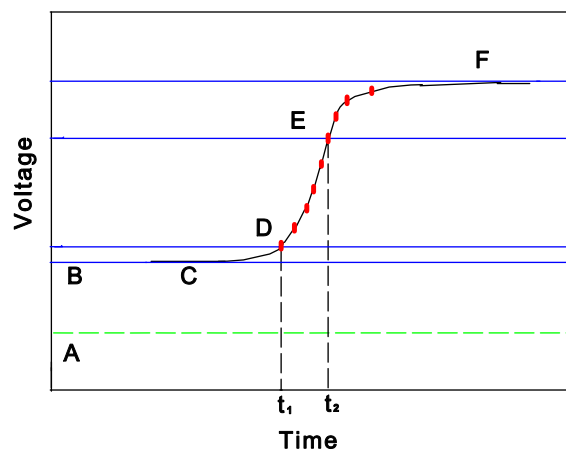


Figure 14 The hypothetical trace showing the voltage of a few hypothetical points. A, Dashed line horizontal cursor that stays at a fixed arbitrary position for the whole period of measurement. B, Solid horizontal cursor that is moved with respect to the dashed line horizontal cursor to show the voltage of each point of the trace. C, Solid cursor showing the voltage of the light-off region. D and E, Solid cursor showing the voltages of the t_1 and t_2 times. F, Solid cursor showing the voltage of the infinite light-on region.

Table 1 Data treatment for transmittance/time at 21 °C.

t (ms)	V (mv)	I_t	I_o	A^a	I_o/I_t	Log A
Light off	-19.2	-	78	-	-	-
50	-24.9	5.7	78	13.6	1.13	0.06
100	-52.7	33.5	78	2.33	0.37	-0.43
150	-80.6	61.4	78	1.27	0.10	-0.98
200	-90.2	71.0	78	1.10	0.04	-1.38
Light-on	-97.2	78.0	78	1.00	0.00	-

^a $A = \log_{10} (I_o/I_t)$.

Thus a calibration plot of $\log_{10} (V_o/V_t)$ against of $[c]$ can be obtained by determining V_o/V_t ratios for various known concentrations of reactant. With respect to the above descriptions, remembering that the difference in voltage output (V) between the light-off and light-on of any obtained trace is proportional to V_o or I_o (C and F regions, Fig. 14), and the difference in voltage output (V) between the light-off and light-on of any obtained trace is proportional to V_o or I_o (C and F regions, Fig. 14), and the difference in voltage output (V) between the light-off and other points of the trace (D and E, Fig. 14) is proportional to V_t or I_t , we can write:

$$V_{\text{light off}} - V_{\text{light on}} \propto I_o$$

$$V_{\text{light off}} - V_D \propto (I_t)_D$$

.

.

.

$$V_{\text{light off}} - V_E \propto (I_t)_E$$

This method was applied to the original oscilloscope Fig. 13 and the relevant data were obtained according to the procedure described in Fig. 14.

These were then converted to give the approximate values for I_o and I_t as reported in the Tables 1 and 2 respectively.

With respect to the kinetic equation $\log_{10} A_t/A_o = -kt/2.303$ two plots of $\log A$ versus time were drawn for the data in Tables 1 and 2. These plots are shown in Fig. 15. The dead-time is the difference in time between the time at which the reaction started (t_o) and the time corresponding to the first observation point (t_1) measured in ms. The dead-time was found by extrapolation from the experimental straight lines. The intersection point of the two experimental straight lines corresponds to the effective start point (t_o) of the reaction. The first experimentally observed points can be seen to be roughly 10 ms later. In this way a dead time (t_o-t_1) of about 10 ms was obtained for the reaction carried out in the refined apparatus shown in Fig. 12.

Table 2 Data treatment for transmittance/time at 23 °C.

t (ms)	V (mv)	I_t	I_o	I_o/I_t	A^a	Log A
Light off	-22.2	-	77	-	-	-
50	-29.4	7.20	77	10.96	1.03	0.01
100	-64.6	42.4	77	1.82	0.26	-0.59
150	-89.2	67.0	77	1.15	0.06	-1.20
200	-93.4	74.0	77	1.04	0.02	-1.76
Light-on	-99.2	77.0	77	1.00	0.00	-

^a $A = \log_{10} (I_o/I_t)$.

3.5. Further improvements to the configuration of the plunger and the spectrophotometer cell

In spite of good progress being made in decreasing the dead-time, it seemed that further reduction could be achieved by modifying the micro-spectrophotometer cell, shown in Fig. 12, to take into account the following points: (i) the reactant volumes of 60 μL were too large, (ii) because the micro-spectrophotometer cell had a height of only 2.5 cm, when the plunger was pushed up in an experiment, some splashing of the solution occurred, (iii) the method of focusing the monitoring light onto the observation area of the cell allowed some stray light to pass through the clear cell walls to the detector. To overcome these difficulties it was necessary to improve still further the configuration of the plunger and the spectrophotometer cell. These changes included: selection of a spectrophotometer cell with walls constructed of black glass to allow more of the light emerging from the LED to be focused on the observation area without stray light reaching the detector; decreasing the height of the exit channel from 10 to 5 mm in order to reduce the time for the mixed reaction to exit from the plunger so reducing the dead time; moving the position of the photodiode to a slightly higher position in comparison with the previous position; improving the configuration of the LED holder to allow the LED to be moved up and down in relation to the photodiode. These modifications are shown in Fig. 16.

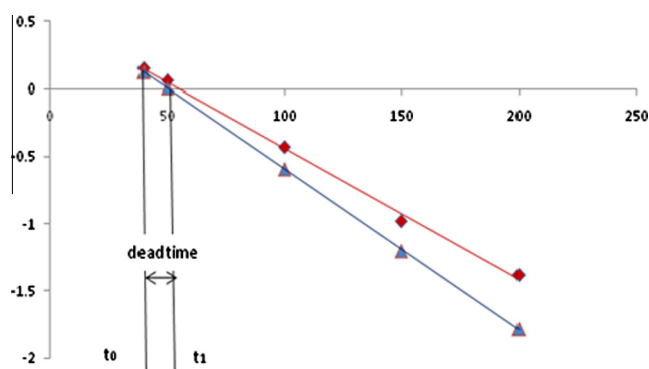


Figure 15 Two plots of $\log A$ versus time (t) for the reduction of 5.0×10^{-4} M DCPI by 5.0×10^{-2} M L-ascorbic acid. Blue line corresponding to the upper trace in Fig. 11 at 23 °C, red line corresponding to the lower trace in Fig. 11 at 21 °C, pH = 5.7 and both the reactants being in 0.1 M phosphate buffer solution.

In a test of the new configuration, two experiments were performed at 17, 21 °C and the reaction was started by the simultaneous injection of 40 μL of each reactant into the mixing cell with the same conditions as in the previous experimental procedure.

Typical oscilloscope trace is shown in Fig. 17 at 21 °C. The treatment to obtain the transmittance/time data corresponding to these traces was as previously described for Fig. 14.

The results are reported in Tables 3 and 4 respectively and two plots of $\log A$ against time are shown in Fig. 18 with respect to the data recorded in Tables 3 and 4. A dead time (t_0-t_1) of about 6.4 ms was obtained from the results of these experiments which indicate that the final attempt to improve the apparatus had successfully reduced the dead time to well

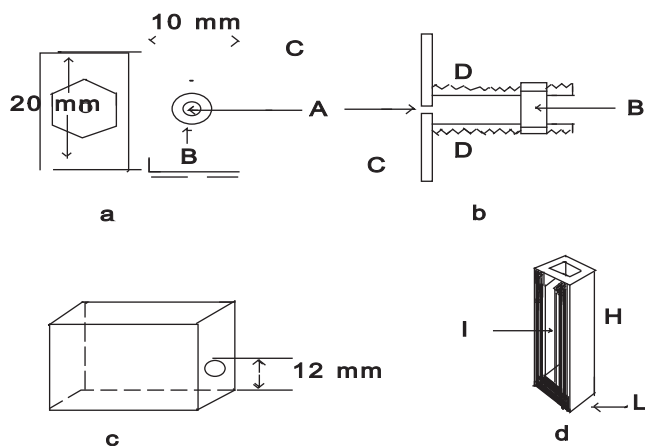


Figure 16 Black cell and holder for the photodiode and LED. (a) Front elevation of LED holder: A, Central hole. B, Hexagonal adjusting nut. (b) Side elevation of LED holder: C, Brass plate. D, Threaded brass tube to hold the LED ($\sim 7\text{--}8$ mm outer diameter and internal diameter to suit the LED). (c) Aluminium holder for the photodiode. (d) Black quartz spectrophotometer cell: I, 2 mm internal width. L, 10 mm path length. H, 45 mm height.

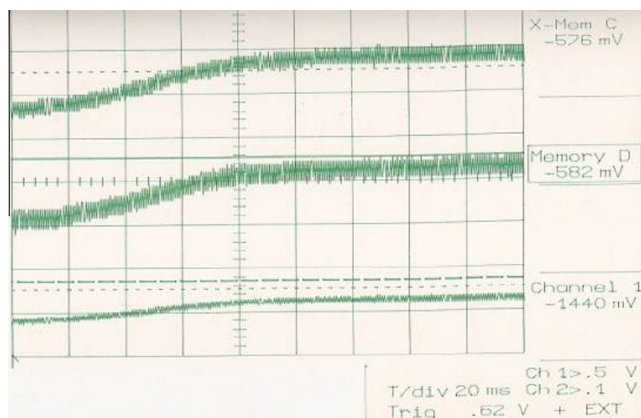


Figure 17 Typical oscillographic picture corresponding to the reduction of 5.0×10^{-4} M DCPI by 5×10^{-2} M L-ascorbic acid when 40 μL of each reactant was mixed at 21 °C and pH 5.7, both the reactants being in 0.1 M phosphate buffer solution. Both upper traces are magnifications of the original lower trace.

Table 3 Data treatment for transmittance/time (t) at 17 °C obtained from relevant trace.

t (ms)	V (mv)	I_t	I_o	I_o/I_t	A^a	$\text{Log } A$
Light off	-190	-	227	-	-	-
10	-197	7	227	32.42	1.51	+0.18
20	-210	20	227	11.35	1.05	+0.02
30	-241	51	227	4.45	0.65	-0.19
40	-276	86	227	2.63	0.42	-0.38
Light-on	-417	227	227	1.00	0.00	-

$$^a A = \log_{10} (I_o/I_t).$$

Table 4 Data treatment for transmittance/time (t) at 21 °C obtained from relevant trace.

t (ms)	V (mv)	I_t	I_o	I_o/I_t	A^a	$\text{Log } A$
Light off	-73	-	228	-	-	-
10	-86	13	228	17.5	1.24	0.095
20	-132	59	228	3.86	0.59	-0.23
30	-191	118	228	1.93	0.29	-0.54
40	-245	172	228	1.32	0.12	-0.91
Light-on	-301	228	228	1.00	0.00	-

$$^a A = \log_{10} (I_o/I_t).$$

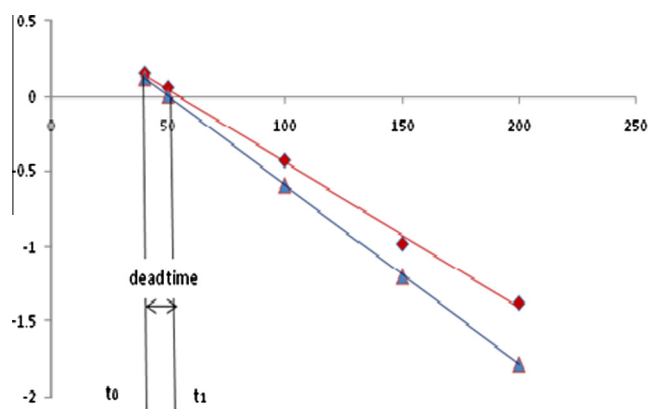


Figure 18 Two plots of $\log A$ versus time (t) for the reduction of 5.0×10^{-4} M DCPI by 5.0×10^{-2} M L-ascorbic acid. Red line corresponding to the relevant trace at 17 °C and pH 5.7. Blue line corresponding to the trace 3 at 21 °C and pH 5.7, both the reactants being in 0.10 M phosphate buffer.

below 10 ms. The equipment could now be used to study reactions with half-lives of 20 ms or longer.

3.6. Further decrease in the dead time of the stopped-flow apparatus

A further decrease in dead time can be obtained if the volumes of the reactants are reduced as much as possible. For this reason, a series of experiments at different temperatures were performed with smaller volumes of the reactants. In separate experiments, 20 μL of each reactant were simultaneously injected into the mixing cell at 19.8, 20.5 and 24.8 °C other con-

Table 5 Data treatment for transmittance/time at 19.8 °C (obtained from its relevant trace).

t (ms)	V (mv)	I_t	I_o	I_o/I_t	A^a	Log A
Light off	-322	-	254	-	-	-
20	-354	32	254	7.94	0.90	-0.05
40	-418	96	254	2.65	0.42	-0.37
60	-482	160	254	1.59	0.20	-0.70
80	-513	202	254	1.26	0.10	-1.00
Light-on	-576	254	254	1.00	0.00	-

$$^a A = \log_{10} (I_o/I_t).$$

Table 6 Data treatment for transmittance/time (t) at 20.5 °C (obtained from its relevant trace).

t (ms)	V (mv)	I_t	I_o	I_o/I_t	A^a	Log A
Light off	-354	-	238	-	-	-
20	-386	32	238	7.44	0.87	-0.06
40	-450	96	238	2.46	0.39	-0.41
60	-512	158	238	1.51	0.18	-0.75
80	-549	218	238	1.09	0.04	-1.40
Light-on	-592	238	238	1.00	0.00	-

$$^a A = \log_{10} (I_o/I_t).$$

Table 7 Data treatment for transmittance/time (t) at 24.8 °C (obtained from its relevant trace).

t (ms)	V (mv)	I_t	I_o	I_o/I_t	A^a	Log A
Light off	-344	-	222	-	-	-
20	-376	32	222	6.94	0.84	-0.08
40	-456	112	222	1.98	0.30	-0.53
60	-520	176	222	1.26	0.10	-1.00
80	-543	204	222	1.09	0.04	-1.45
Light-on	-566	222	222	1.00	0.00	-

$$^a A = \log_{10} (I_o/I_t).$$

ditions being as previously stated. Typical oscillographic traces were obtained and the data treatment for transmittance/time corresponding to these original oscilloscope traces is reported in Tables 5–7. Three plots of $\log A$ versus time (t) were drawn with respect to the data recorded in Tables 5–7 (corresponding to their relevant traces). These plots are shown in Fig. 19. In this way a dead time (t_0-t_1) of about 3.4 ms was determined for the final modified form of the stopped-flow apparatus.

3.7. Determination of the pseudo first-order rate constants for the reaction between DCPI and L-ascorbic acid

From the results obtained from the final set of experiments (Fig. 19), the slope of each plot can be calculated as the change of $\log_{10} A$ divided by the change of the time as:

$$\text{Slope} = \Delta \log_{10} A / \Delta t$$

This slope is equal to the theoretical slope of the integrated first order equation $\log_{10} A/A_o = -(k/2.303)t$, and may be shown as:

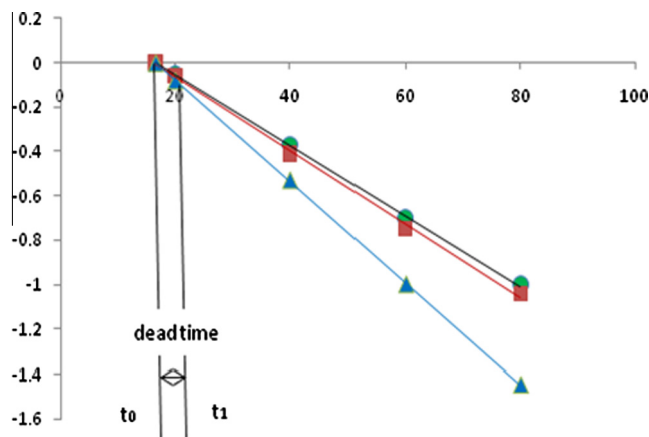


Figure 19 Three plots of $\log A$ versus time (t) for reduction of 5.0×10^{-4} M DCPI by 5.0×10^{-2} M L-ascorbic acid at pH 5.7. Green plot corresponding to the relevant trace at 20.5 °C. Red plot corresponding to the relevant trace at 24.8 °C, both the reactants being in 0.1 M phosphate buffer solution.

Table 8 Showing the experimental pseudo first-order rate constants ($k = -2.303.S$) for the reduction of DCPI by L-ascorbic acid at pH 5.7.

T (°C)	t_1 (ms)	t_2 (ms)	$\log A_1$	$\log A_2$	$S = \Delta \log A / \Delta t$	k (s^{-1})
19.8	47.6	35.2	-0.5	-0.3	-0.2/12.4	37.15
20.5	45.6	34.0	-0.5	-0.3	-0.2/11.6	39.71
22.4	42.3	31.8	-0.5	-0.3	-0.2/10.5	46.77
24.8	38.0	29.6	-0.5	-0.3	-0.2/8.4	54.83

$$\Delta \log_{10} A / \Delta t = -k / 2.303 \text{ or } k = -2.303 \times \Delta \log_{10} A / \Delta t$$

Thus, the relevant values of the pseudo first-order rate constant (k) can be easily calculated from the calculated values of the $\Delta \log A / \Delta t$ ratio. This ratio is measurable for any two arbitrary points (e.g. $\log A_1 = -0.5$ and $\log A_2 = -0.3$) of each plot, and they are reported in Table 8.

In the temperature range studied the dependence of the rate constants on temperature was in agreement with the Arrhenius equation:

$$\log k = -E_a / (2.303 \times R) \times (1/T) + \text{constant}$$

(E_a = activation energy, T = Temperature (Kelvin), R = gas constant), as can be seen from Table 9 and Fig. 20 respectively. Table 9 also provides values for the reaction half-life at the respective temperatures. This good linear dependence is another demonstration of the efficiency of the apparatus. The activation energy of the process studied can be calculated from the slope of the Arrhenius plot via slope = $-E_a / (2.303 R)$. This slope is measurable for any two arbitrary points (e.g. $\log k_1 = 1.67$ and $\log k_2 = 1.73$) of the plot and can be written as: slope = $(1.67-1.73) / (3.38-3.36) \times 10^3 = -3 \times 10^3$ and $E_a = 3.10^3 \times 2.303 \times 8.3 \times 10^{-3} = 57.3 \text{ kJ mol}^{-1}$.

Table 9 Effect of temperature on the pseudo first-order rate constant for the reduction of DCPI by L-ascorbic acid at pH 5.7.

T (K)	k (s^{-1})	$\log k$	$1/T$ (K^{-1}) ($\times 10^{-3}$)	$t_{1/2}(\text{ms}) = \text{Ln } 2/k$
19.8 + 273.15	37.15	1.57	3.41	18.7
20.5 + 273.15	39.71	1.60	3.40	17.5
22.4 + 273.15	46.77	1.67	3.38	14.8
24.8 + 273.15	54.83	1.74	3.35	12.6

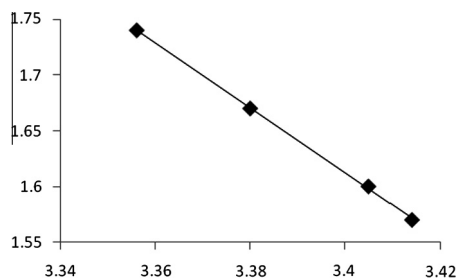


Figure 20 Dependence of the pseudo first-order rate constant on reciprocal temperature in accordance with the Arrhenius equation for the reduction of DCPI by L-ascorbic acid.

3.8. Second order rate constant for the reaction between DCPI and L-ascorbic acid

To obtain a second order kinetic constant (k') for the reaction between 5×10^{-4} M DCPI and 5×10^{-2} M L-ascorbic acid for the final set of present work (Fig. 19), the experimental pseudo first order rate constant $k = 54.8 \text{ s}^{-1}$ was obtained at pH 5.7 and 24.8°C (Table 8). This together with the concentration of L-ascorbic acid in mixing chamber allowed the second order rate constant ($k' = k / [\text{L-ascorbic acid}]$) to be estimated as follows:

$$k' = k / [\text{L-ascorbic acid}] \quad k' = \{54.8 \text{ s}^{-1} / (5 \times 10^{-2} \text{ M} / 2)\} \\ = 2192 \text{ s}^{-1} \text{ M}^{-1}$$

It is important to remember that in the present work the concentration of each reactant in the mixing chamber is half that of the concentration in the syringe (the stopped-flow apparatus uses syringes of equal volume). Hence, the above value of second order rate constant (k') is based on the concentration of L-ascorbic acid in the mixing chamber ($5 \times 10^{-2} \text{ M} / 2$). To compare the second order rate constant obtained from the present study with Tonomura's study (Tonomura et al., 1978), the pseudo first order rate constants obtained from the Tonomura's study for the reduction of 4.0×10^{-4} M DCPI by 2.0×10^{-2} M L-ascorbic acid in the mixing chamber are reported in Table 10 and the plot of $\log k$ versus pH is also shown in Fig. 21.

From Fig. 21, showing Tonomura and Nakatani's results, the value of the pseudo first order constant ($k = 45.7 \text{ s}^{-1}$) at pH 5.7 was interpolated. This together with the concentration of ascorbic acid in mixing chamber (4.0×10^{-4} M), allowed the second order rate constant at pH 5.7 ($k' = k / [\text{ascorbic acid}]$) to be estimated. In Table 11, this value is compared with the value obtained for the data obtained in the present work. These two values for the second order rate constant are in good agreement and indicate that the current apparatus functioned satisfactorily.

Table 10 Effect of the pH on the pseudo first order rate constant (k) for the reduction of DCPI by L-ascorbic acid at 25°C (Tonomura et al., 1978).

pH	k (s^{-1})	$\log k$	$t_{1/2}(\text{ms}) = \text{Ln } 2/k$
2.03	1028	3.01	0.674
4.07	837	2.92	0.830
4.91	224	2.35	3.09
6.07	24.1	1.38	28.00

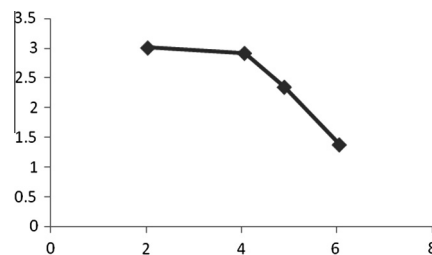


Figure 21 Dependence of the pseudo first-order rate constant on reciprocal temperature in accordance with the Arrhenius equation for the reduction of DCPI by L-ascorbic acid.

Table 11 Value of second order rate constant of present work and Tonomura's work (Tonomura et al., 1978) for reaction between DCPI and L-ascorbic acid.

	k (s^{-1})	$k'/s^{-1} \text{ M}^{-1} = k/[\text{ascorbic acid}]$	T ($^\circ\text{C}$)
Tonomura's work	45.7	2285	25.0
This work	54.8	2192	24.8

3.9. Mixing test

Since, in the stopped-flow method, the reaction is started by mixing two solutions, mixing efficiency is one of the most fundamental factors involved in the correct estimation of rate constants. Incomplete mixing may lead to underestimation of the rate constant. In this work, the mixing efficiency of the apparatus was evaluated by mixing a solution of sodium hydroxide with a solution of hydrochloric acid of concentration just sufficient to change the colour of the pH indicator bromothymol blue from yellow to blue. Neutralisation and proton transfer reactions are in general extremely fast (Eigen and Hames, 1960), and hence, any unchanged (i.e. still yellow) indicator appearing in the observation cell will be the result of incomplete mixing.

The original oscilloscope pictures are shown in Figs. 11, 22 and 23 respectively. Fig. 11 shows the mixing of water with water. Fig. 22 shows the mixing of (HCl/bromothymol blue) with water. It will be seen that there is as expected a small drop in transmission of the mixed solution compared with water/water. Fig. 23 shows the mixing of (HCl/bromothymol blue) with NaOH solution. A large drop in transmission is seen due to the absorption of the monitoring light by the blue solution. Comparison of Figs. 22 and 23 shows that the change from the yellow form of the indicator to the blue form is

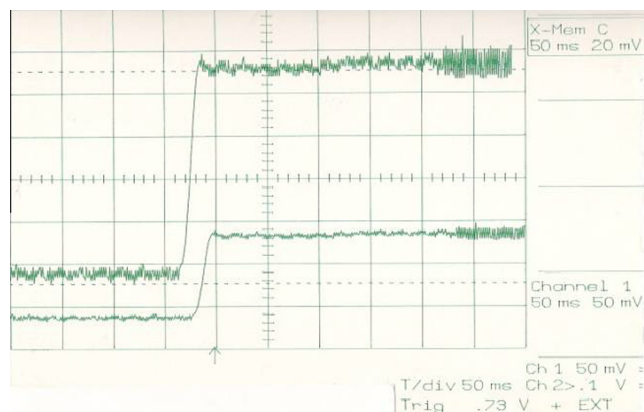


Figure 22 Typical oscillographic picture obtained when 20 μL of 0.009 N HCl containing bromothymol blue indicator was mixed with 20 μL of water. Upper trace is a magnification trace of lower trace.

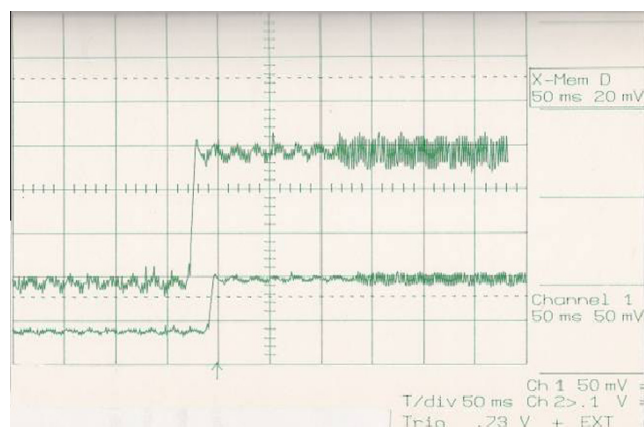


Figure 23 Typical oscillographic picture obtained when 20 μL of 0.009 M HCl containing bromothymol blue indicator was mixed with 20 μL of 0.01 M NaOH. The upper trace is a magnification of the lower trace.

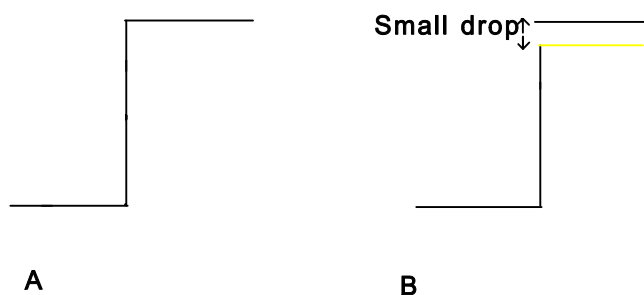


Figure 24 Increase in transmission due to the sudden rise in the plunger on mixing (B): a solution of the HCl and bromothymol blue (yellow form) with water (A): water and water. In (B) the increase in transmission is less due to the small absorbance of the yellow form of the indicator at the monitoring wavelength.

largely complete (92.5%) within the dead time of the apparatus. It takes only a further 3 ms for mixing to be complete. Figs. 24 and 25 reveal how these changes occurred in the original oscilloscope pictures 11, 22 and 23.

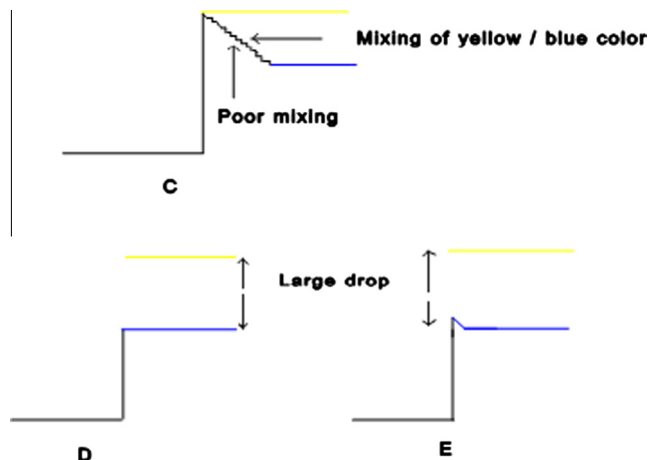


Figure 25 A large drop in transmission of the mixed solution of (HCl/bromothymol blue) and NaOH due to the absorption of the monitoring light by the blue form of indicator (C, D and E cases) compared with a small drop in transmission of the mixed solution of (HCl/bromothymol blue) and water (B case, FIG. 24). C, Mixing of (HCl/bromothymol blue) and NaOH when the mixing efficiency of the apparatus is extremely poor (takes longer than the dead time). D, Mixing of (HCl/bromothymol blue) and NaOH when the mixing efficiency is ideal (100% mixing within the dead time). E, Mixing of (HCl/bromothymol blue) with NaOH solution in the stopped-flow apparatus for this study (92.5% mixing within the dead time). In each case the yellow line represents the transmission level that is obtained if water is used in place of NaOH.

4. Conclusion

As mentioned previously, one of the most important factors affecting the performance of a stopped-flow apparatus is the “dead-time”. Another definition of dead time t_d is the time required for solution to flow from the centre of the mixing volume to the centre of the observation cell; the change occurring in the reaction mixture cannot be observed during t_d . If we define the dead volume V_d (ml) as the volume of dead space between the centre of the mixer and the centre of the cell, the dead time (s) is written by Hiromi (1980):

$$t_d = V_d/U \quad (1)$$

where U is the flow velocity in millilitres per second.

The observable fraction of a change due to the reaction, with an apparatus of a given dead time, is determined by the relative magnitude of the dead time with respect to the reaction half-life, $t_{1/2} = 0.693/k$ for first order reaction. For a first order reaction the relationship between the observable fraction (f_{obs}) of total reaction and the dead time of the apparatus is given by Hiromi (1980):

$$f_{\text{obs}} = (1/2)^{t_d/t_{1/2}} \quad (2)$$

The relationship between the dead time measured during this study k and the observable fraction (f_{obs}) of the reaction between DCPI and L-ascorbic acid, performed at 19.8 $^{\circ}\text{C}$ ($k = 37.15 \text{ s}^{-1}$), is reported in Table 12. This table shows why the shortening of the dead-time is so important to improve the performance of the stopped-flow apparatus.

Table 12 Relationship between the observable fraction (f_{obs}) of the total reaction between the DCPI and L-ascorbic acid ($k = 37.15 \text{ s}^{-1}$) and the dead-time (t_d).

t_d (ms)	f_{obs} (%)
50 (approx.)	1.6
10	69.5
6.4	78.9
3.4	87.7

Table 13 Relationship between the volume of each reactant and the dead-times determined in this work.

Volume of each reactant (μL)	Dead-time (ms)
300	50 (approx.)
60	10
40	6.4
20	3.4

Decreasing the dead-time from 50 to 3.4 ms increased the fraction of observable reaction from 1.6% to 87.7%. From the optimisation information obtained from these experiments it appears that the dead time can be reduced by decreasing both the volume of reactants and the dead volume (Eq. (1)). For all the experiments, as described previously, the relationship between the volumes of each reactant and the dead-time of the apparatus is reported in the Table 13.

As the Table 13 indicates, the decrease in the dead-time is approximately proportional to the reduction of the volume of each reactant; thus the dead-time of initial apparatus can be estimated to be about 50 ms. Preliminary observations also indicate that more rapid mixing with smaller volumes and greater monitoring sensitivity may be possible by modification of the size of the observation area. To improve overall instrumental performance, it is necessary to make the following changes: increase in the intensity and stability of the light source; improvement in the optical system to focus more of the light through the observation cell; employment of a more sensitive and stable detection system; decrease in the size of the mixing chamber in the plunger; decrease of the volume of the observation area by using smaller reactant volumes. However, volumes of reactants less than 20 μL (total) are not practical because of incomplete mixing (Richard, 1969) also an extremely small observation cell would reduce the intensity of the light reaching the photodiode and frequently would result in an unacceptable signal-to-noise ratio. Increase of the flow velocity by means of a pneumatic or hydraulic device to drive the solutions into the mixer would reduce the dead time of the apparatus. However, this requirement also has limitations; for example, a high flow velocity may give rise to "cavitation" which is the bubbling of dissolved gas during flow and after stopping. These changes have altogether the potential to provide a high performance stopped-flow apparatus with a dead-time of less than 3.5 ms. At present, some types of stopped-flow instrument have a dead time as short as 0.5 ms or less (Berger et al., 1968). In this case, the reduction of 2,6-

dichlorophenolindophenol by L-ascorbic acid (Tonomura et al., 1978) at pH 2 is recommended as the most practical test for checking the performance of the apparatus.

Acknowledgements

We gratefully acknowledge financial support from the Universities of Salford and Sistan & Baluchestan.

References

- Andrea, B., Giovanni, A., Maurizio, B., 1990. *J. Biol. Chem.* 256, 18898–18901.
- Berger, R.L., Balko, B., Borchardt, W., Friauf, W., 1968. *Rev. Sci. Instrum.* 39, 486–493.
- Brzovic, P.S., Dunn, M.F., 1993. In: *Bioanalytical Instrumentation*, vol. 37. J. Wiley & Sons Inc., New York, p. 191.
- Brzovic, P.S., Dunn, M.F., 1995. In: *Methods in Enzymology*, vol. 246. Academic Press, p. 168.
- Chance, B., Franklin, 1940. *J. Inst.* 229, 455–766.
- Coolen, R.B., Papadakis, N., Avery, J., Enke, C.G., Dye, J.L., 1975. *Anal. Chem.* 47 (9), 1649–1655.
- Dye, J.L., Feldman, L.H.R., 1966. *Rev. Sci. Instrum.* 37 (2), 154–157.
- Eigen, M., Hames, G.G., 1960. *J. Amer. Chem. Soc.* 82 (22), 5951–5952.
- Gibson, Q.H., 1966. *Ann. Rev. Biochem.* 35, 435–456.
- Gibson, Q.H., Greenwood, C.J., 1963. *Biochem. J.* 86 (3), 541–544.
- Gibson, Q.H., Eisenhardt, R.H., Chance, B., LonbergHolm, K.K., 1964. *Rapid Mixing and Sampling Techniques in Biochemistry*. Academic Press, New York.
- Giovanni, A., Andrea, B., Antonio, C., Giancarlo, F., Maurizio, B., 1994. *Acta* 1205 (2), 252–257.
- Hartridge, H., Roughton, F.J.W., 1923. The rate of binding of carbon monoxide to hemoglobin. *Proc. Roy. Soc. (London)* A104, 376.
- Hiromi, K., 1980. In: Glick, D. (Ed.), *Method of Biochemical Analysis*, vol. 26. John Wiley & Sons, New York, pp. 137–164.
- Ishihara, K., Kondo, Y., Koizumi, M., 1999. *Rev. Sci. Instrum.* 70, 244.
- Kahl, V., Gansen, A., Galneder, R., Rädler, J.O., 2009. *Rev. Sci. Instrum.* 80 (07), 3704.
- Milano, M.J., Pardue, H.L., 1975. *Anal. chem.* 47 (1), 25–29.
- Nakamura, T.J., 1971. A new flow apparatus for steady and stopped-flow measurements. *Biochem. (Tokyo)* 70, 961–966.
- Paradakis, N., Coolen, R.B., Dye, J.L., 1975. *Anal. Chem.* 47 (9), 1644–1649.
- Richard, A.H., 1969. *Anal. Biochem.* 29 (1), 58–67.
- Ridder, G.M., Margerum, D.W., 1977. *Anal. Chem.* 49 (13), 2098–2108.
- Sienkiewicz, A., Qu, K., Scholes, C.P., 1994. *Rev. Sci. Instrum.* 65, 68.
- Suelter, C.H., Coolen, R.B., Dye, J.L., 1975. *Anal. Biochem.* 69 (1), 155–163.
- Tjahjono, M., Davis, Th., Garland, M., 2007. *Rev. Sci. Instrum.* 78 (02), 3902.
- Tonomura, B., Nakatani, H., Ohnishi, M., Yamaguchi-Ito, J., Hiromi, K., 1978. *Anal. Biochem.* 84 (2), 370–383.
- Wightman, R.M., Scott, R.L., Reilly, C.N., Murray, R.W., Burnett, J.N., 1974. *Anal. Chem.* 46 (11), 1492–1499.
- Yutaka, O.J., 1984. *Biol. Chem.* 259, 7187–7190.